Original and strengthened traditional timber connections

J.M. Branco & P.J. Cruz
ISISE, University of Minho, Portugal

M. Piazza
University of Trento, Trento, Italy

ABSTRACT: A series of monotonic and cyclic tests on unstrengthened full-scale specimens were performed in order to characterize the original behavior of connections representative of traditional timber trusses. Subsequently, connections strengthened with metal devices were tested under monotonic and cyclic loading. Tests on assembled connections were preceded by accurate material characterization, in terms of the mechanical properties of the timber elements used for all full-scale models. The experimental study was complemented by a numerical analysis using FEM, through parametric studies that followed the models calibration process.

1 INTRODUCTION

Joints on traditional timber structures are normally made by notches where stresses are directly transferred by compression and/or friction between the surfaces in contact. In the oldest cases, notched joints present tenon and mortise to ensure the perfect contact between the connected elements and to prevent the out-of-plane instability. In the more recent examples, as a cause-effect of the reduction of available carpenters, tenon and mortise have been substituted by metal devices. In addition, the joints strengthening with bolts, stirrups, binding strip, etc. provides an important improvement in the overall structural behavior under seismic actions by ensuring safety under reversal loads.

Traditional timber connections, even without any strengthening device, usually have a significant moment-resisting capacity. Therefore, they cannot be represented by common constraints models like perfect hinges or rigid joints. Their common design method looks out only to the strength characteristics. However, as traditional timber structures are highly indeterminate, the real behavior of joints has an important influence on the force distribution.

2 EXPERIMENTAL CAMPAIGN

The experimental research was carried out at the Laboratory of Structures of the University of Minho, and includes monotonic and cyclic tests of full-scale traditional timber connections. A series of monotonic and cyclic tests on unstrengthened specimens were performed in order to study the primary behavior characteristics of the connection, as well as its sensitivity to a few parameters. Subsequently, connections strengthened with basic metal devices were tested under monotonic and cyclic loading. The purpose of these tests was to uncover any advantages and deficiencies in the behavior of the joint and of the device itself, as well as to determine a need for different types of strengthening. Tests on assembled connections were preceded by accurate material characterization, determining the mechanical properties of the timber elements used for all full-scale models.

Because of their frequency in the preliminary survey undertaken, two skew angles of the connections were adopted: 30° and 60°. Two compression levels of the rafter were adopted, 1.4 MPa and 2.5 MPa, in accordance with the Service and Ultimate Limit States, respectively, defined for common Portuguese timber roof structures (Branco, 2008). For all type of connection evaluated, nine tests were performed: 6 monotonic, 3 in each loading direction (positive and negative) and 3 others under cyclic loading. Strengthened connections were studied only under a compression level in the rafter of 1.4 MPa corresponding to the Service Limit State conditions. Four strengthening techniques were initially selected but, during the experimental campaign one of them was abandoned.

2.1 *Test setup and instrumentation*

The arrangement allows independent control of two hydraulic jacks (Fig. 1). One jack, aligned with the rafter, induced constant compression throughout the test. The other, a double-acting jack, positioned above the center of the joint, applied a transversal force, with a programmed load cycle, and generated a moment at the joint. Force (F) versus displacement (d) curves was measured. The two jacks have a maximum loading capacity of 50 kN and 100 kN and a maximum stroke of 160 mm and 50 mm, respectively.

Type and location of instrumental channels, including load cells and LVDT, are shown in Figure 1.
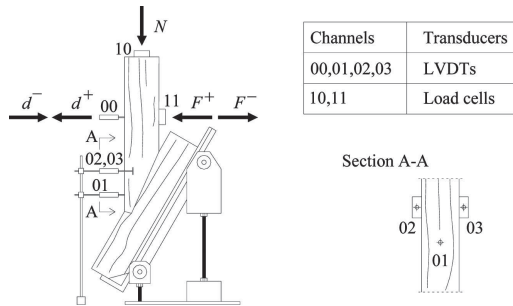
Figure 1. Testing apparatus and instrumentation layout.

Channels	Transducers
00,01,02,03	LVDTs
10,11	Load cells

(a) Stirrups (b) Internal bolt

(c) Binding strip (d) Tension ties

Figure 2. Traditional strengthening techniques evaluated.

Tests were performed under displacement control for the typical birdsmouth joint skew angle of 30° and 60°. For all the specimens, the cross sections of the elements were 80×220 mm^2, the step depth was 45 mm and the notch length was 422 mm.

The first step of the loading procedures in both the monotonic and cyclic tests was the application of an axial compression force on the rafter. The axial force, simulating the effect of the dead load presented in the structure, was kept constant during the test. In the subsequent loading steps, a transversal force (F), acts perpendicular to the rafter axis. When the skew angle increases, it is defined as the positive direction and when the skew angle decreases, it is defined as the negative direction.

Monotonic tests were performed to determine the elastic behavior, in particular, the apparent elastic limit displacement d_e^+ and d_e^-. Under displacement control at channel 00, a maximum displacement value of 50 mm, was imposed under a movement rate of 0.028 mm/s and 0.18 mm/s in the case of connections with a skew angle of 30° and 60°, respectively.

2.2 Cyclic test procedure

Full-scale connections, similar to the specimens of monotonic loading, were tested with a quasi static cyclic loading. In particular, the test program included one cycle in the range [0.25 d_e^+; 0.25 d_e^-]; one cycle in the range [0.50 d_e^+; 0.50 d_e^-]; three cycles in the range [0.75 d_e^+; 0.75 d_e^-]; three cycles in the range [n d_e^+; n d_e^-] until joints failure. The values used for the elastic limit displacements, for both positive (d_e^+) and negative (d_e^-) directions, are based on results obtained in the monotonic tests.

2.3 Strengthening techniques studied

The four basic types of intervention considered in this study are modern implementations of traditional strengthening techniques: the stirrups, the internal bolt, the binding strip and the tension ties (Fig. 2).

Metal stirrups placed in pairs at two opposite sides of the joint were very popular in the past and are still considered adequate and frequently adopted. The effect of the large increase of in-plane stiffness con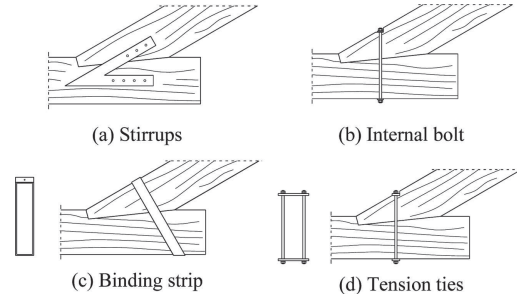nection is particularly important and should be investigated. In this study, each stirrup was composed of two steel plates welded in a V-shape. Each prong was 50 mm wide and 5 mm thick. They were parallel to the rafter or to the tie beam, and bolted to it with seven bolts of 10 mm diameter. The use of a steel rod, with 12 mm diameter, was also considered. The rod was fixed by a nut at both ends and secured by using a special rectangular-shape washer (70×30 mm^2 and 5 mm thick). The rod was located at the mid-joint and normal to the axis of the tie beam. A suitable seat area was formed in the rafter for accommodating it, which allows perfect contact between surfaces.

Metal binding strips, considered obsolete today, were very frequently adopted in the 19th century roof structures, particularly to strengthen the rafter and tie beam connection in configurations that had skew angles typically of 30°, see Branco (2008). Two updated versions of this layout were considered: a) the joint was bound with a hollow steel ribbon, 50 mm wide and 5 mm thick, located at mid-joint, normal to the tie beam (BSi); b) the joint was bound with two steel plates located in the bottom surface of the tie beam and upper surface of the rafter, with the dimensions of 40×159 mm^2 and 10 mm thick, tightened through two rods of 12 mm (TTi). The rods, having a nut at both ends, located at midjoint, normal to the tie beam, enable full control in the tightening force during the strengthening lifetime. The first version, called rigid binding strip, was only used for 30° skew angle case.

2.4 Analysis and discussion of the tests results

The first set of connections tested was composed by three unstrengthened joints with a skew angle of 30° (U3-1.4-1,2 and 3). A permanent compression force of 25 kN (corresponding to 1.4 MPa compression stress) was applied to the rafter throughout the vertical jack, and the second jack imposed a monotonic transversal force (perpendicular to rafter axis). The test results illustrate perfect elastic-plastic behavior for the three tests (Fig. 3). The behavior is perfectly elastic until the elastic limit displacement (approx 8 mm) is reached, thus the behavior became non-linear but only within a small range. Subsequently, a quasi-perfect plastic behavior appears. This pseudo-plastic phase, starting at a 10 mm displacement, remains practically constant
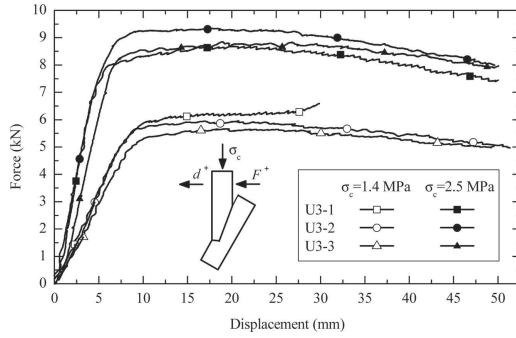
Figure 3. Force-displacement curves of unstrengthened connections with 30° skew angle for monotonic loading in positive direction and different rafter compression stress.
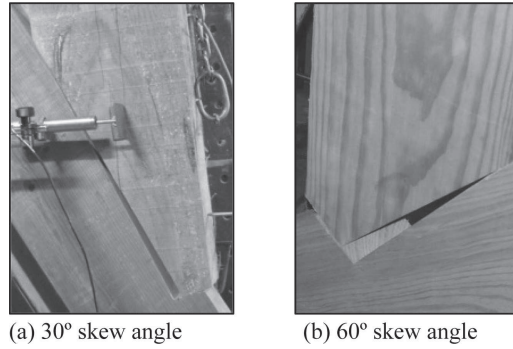

(a) 30º skew angle (b) 60º skew angle

Figure 4. Slip mechanism observed when decreasing the skew angle (negative direction).
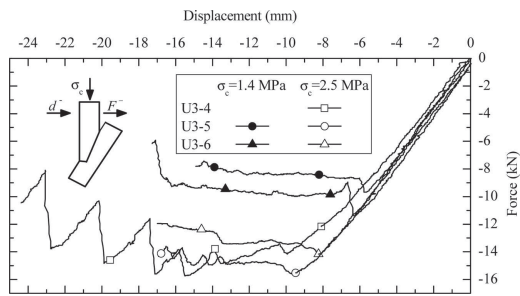

Figure 5. Force-displacement curves of unstrengthened connections with 30° skew angle for monotonic loading in negative direction and different rafter compression stress.

until the maximum displacement (50 mm), presenting a small decrease of the resistance after 25 mm displacement. The subsequent sets of tests aim to evaluate the influence of the compression stress level applied to the rafter.

Comparing the force-displacement of the two different compression level considered, apart of an increased in the maximum force also a higher stiffness is achieved with the increase of the compression level (Fig. 3). With the increment of the rafter compression stress, the stiffness more than duplicate, the maximum force reached is 61.3% higher but the elastic displacement limit decreases 34.2%. However, the development of the force-displacement curves remains similar.

A more brittle behavior and excessively depending of the friction conditions were detected when the skew angle is reduced. The curves presented in Figure 5 show a perfectly elastic behavior just at the maximum force, after which a slip, followed by a loss of friction, induces a rapid decrease of the resistance. When the new stable position of the joint is reached, the brittle behavior is replaced by a pseudo-plastic phase. This ductile behavior is due to the local compression of wood. Finally, a total loss of friction occurs with the failure of the connection.

Comparing the force-displacement curves obtained for the two different rafter compression stress considered, under the same transverse loading history (negative field), only an increase in the maximum force and corresponding elastic limit displacement can be pointed out (Fig. 5). The same brittle behavior after the elastic displacement limit is observed. The development of the force-displacement curves, in particular their stiffness characteristics, remains constant.

Comparing the force-displacement curves obtained for both rafter compression stress levels, under monotonic loading in positive and negative directions important conclusions can be pointed out. First, the behavior is quite asymmetric. The elasto-plastic behavior presented in the positive direction became brittle and more depending of the friction conditions in the negative direction. This difference is a consequence of the distinct mechanism developed, in particular, the ductile

behavior of wood under compression, contrary to the fragile behavior characteristic of the friction conditions that stipule the behavior in the negative loading direction. No failure is reached in the positive loading direction while in the negative one, an early failure happen near the 15–20 mm of displacement. For a rafter compression stress of 1.4 MPa, the stiffness and the maximum force obtained for the positive loading direction represents 50% of the ones measured in the negative field. However, the behavior in the positive loading direction is more ductile, allows higher displacements and elastic limits. In the case of a rafter compression stress equal to 2.5 MPa, the stiffness is very similar but the maximum force is higher in the negative loading direction.

The asymmetric behavior observed under monotonic loading for unstrengthened connections with 30° and 60° skew angles, as result of the different resistant mechanism in each direction, has consequences in the behavior under cyclic loading. The obtained response is asymmetric (Fig. 6). Energy dissipation occurs only in the negative direction. However, the force-displacement curves show a non-linear development in both directions. This energy dissipation is mainly produced by the sliding of the rafter when pulled into the negative direction. Increasing the rafter compression stress, the force-displacement curves shape remains similar, presenting an increment in the maximum force values. With the rafter compression stress,
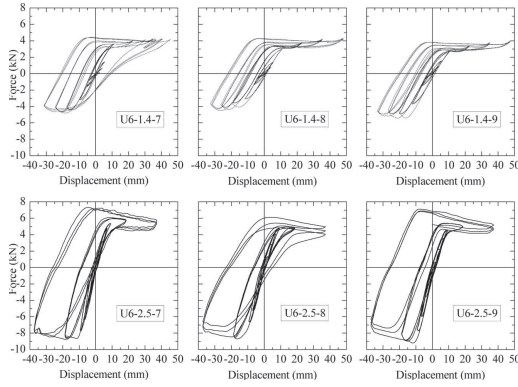
Figure 6. Force-displacement curves of unstrengthened connections with 60° skew angle under cyclic loading for different rafter compression stress.
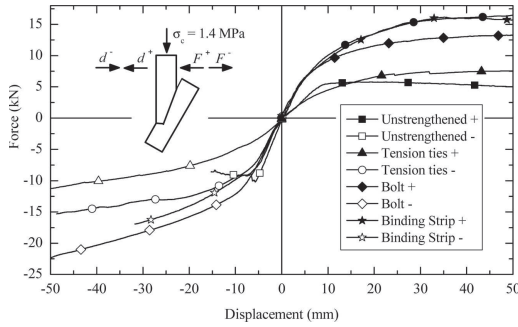

Figure 7. Force-displacement curves for unstrengthened and strengthened connections with 30° skew angle under monotonic loading.

Figure 8. Force-displacement loops for unstrengthened and strengthened connections with 60° skew angle under cyclic loading.

the energy dissipation and the equivalent viscous damping ratio (V_{eq}) grow from 2.45% to 3.96% and from 23.40% to 36.00%, respectively. Nevertheless, the higher increase is due to the skew angle enlarge from 30° to 60°. The main difference between the rafter compression stresses applied was that, for 1.4 MPa, no failure was reached, while, with 2.5 MPa, all three specimens presented damage.

2.5 Strengthening conclusions and comparisons

Comparing the experimental force-displacement curves, obtained for the unstrengthened and strengthened connections, it is recognized that all the strengthening schemes improve the behavior of the originals connections (Fig. 7).

The elasto-plastic behavior with limited ductility evidenced by the unstrengthened connections under negative loading direction is substituted by full non linear curves exhibiting high ductility in the strengthened connections. Comparing the strengthening techniques evaluated, the less efficient (maximum force and stiffness), is the tension ties.

Connections strengthened with stirrups and binding strip attained the same range of maximum force,
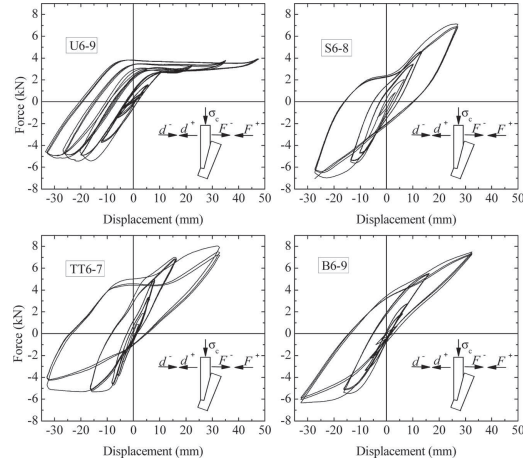
however, this later scheme has a lower ductility capacity. In particular, the maximum resistance for the strengthened connections with stirrups and internal bolt is achieved near the end of the test. However, in the strengthened connections with binding strip, when the tests were interrupted, the force value was already decreased. Therefore, between the internal bolt and the binding strip, the first one is more efficient in terms of ductility capacity with the goal to assure a better seismic behavior of the connection. The effect of the strengthening schemes in the negative loading directions of the monotonic tests is obvious: the increase of the maximum force and of the ductility capacity. The benefits to the stiffness are not significant (the stiffness exhibit by the tension ties technique is even minor).

The improvements in the connections behavior under monotonic loading, provided by the strengthening techniques evaluated are highlight by the response under cyclic loading. Without any strengthening device, the connection is not able to prevent the failure causes by load reversals (detachment of the connected elements) even when the rafter compression stress is augmented (from 1.4 MPa to 2.5 MPa). The unstrengthened connections showed a very limited capability to dissipate energy. All strengthening techniques adopted were efficient in the improvement of the hysteretic behavior of the connections. The best results under cyclic loading are achieved when the stirrup, bolt and tension ties techniques are used. The binding strip provides the strongest connections but the equivalent damping ratio is nearly half of the values presented by the others strengthened connections.

In the case of 60° skew angle, the strengthening techniques evaluated provide a force-displacement behavior more stable (Fig. 8). More cycles are achieved, the pinching effect of the unstrengthened connections is reduced and a more symmetric response is obtained.
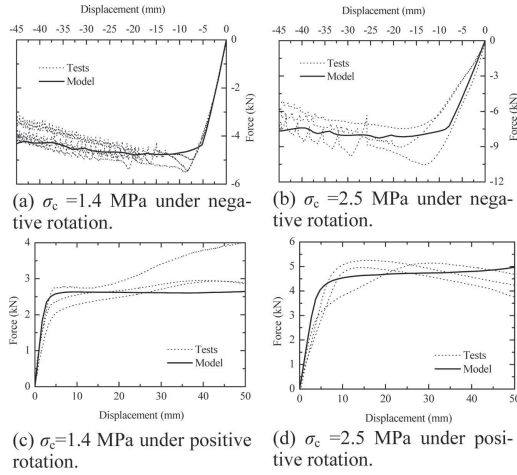
(a) σ_c =1.4 MPa under negative rotation.

(b) σ_c =2.5 MPa under negative rotation.

(c) σ_c=1.4 MPa under positive rotation.

(d) σ_c =2.5 MPa under positive rotation.

Figure 9. Comparison between experimental and numerical force-displacement curves (60° skew angles).

3 NUMERICAL MODELLING

The tests results on full-scale specimens became the fundamental reference for the subsequent step of the research: finite element modeling of unstrengthened connections. Bi-dimensional models were set up using the commercial package (Abaqus, 2007). The geometry and loading of the connections permits the assumption of a state of plane stress for the model.

3.1 Model

The adopted finite element mesh used quadrilateral plane 8-node elements (named by the software package as CPS8R) considering a strain thickness of 80 mm. The key element of the finite element model (FEM) used is the interaction between the two wood elements (rafter-tie beam). The overall response of the joint is highly dependent of the behavior adopted for the interaction. The interaction was modeled assuming a surface-to-surface contact. For that, the notch surface of the tie beam was considered as master surface and the notch surface of the rafter as the slave. For the sliding formulation, *finite sliding* formulation (Oden & Pires, 1983), based on the node-to-surface discretization method was taken on. Due to the rotational movement applied to the connections, the contact surfaces must be extended to outside the limits of the original contact surface.

Friction, along with tangential constraints or relative displacements between contact surfaces, was implemented with reference to Coulomb's friction model after an appropriate choice of friction coefficients. By default, a value of 0.2 was used for the friction developed in the interaction however, a sensitivity study, which the results are presented in next sections, was performed to evaluate the influence of this parameter in the joint behavior.

3.2 Numerical vs. experimental results

Tests results were used to calibrate the numerical models for 30° and 60° skew angles. Results are expressed in terms of force-displacement curves, evaluated at the same location and under the same load history as the tests.

As example, Figure 9 compares behavior curves obtained with the numerical model calibrated for the case of 60° skew angle and for both compression level in the rafter $\sigma_c = 1.4$ MPa and $\sigma_c = 2.5$ MPa) with the tests results.

In general, the numerical analysis seems to supply satisfactory information about the joint behavior. Despite some difference, numerical models show to be adequately fitted to the experimental results. The accuracy of the models increases significantly under negative rotation. In this situation, the mechanism of reaction is soon concentrated in a highly compressed zone. The joint behavior depends of friction, as described below. Friction acts in the front notch surface, with a real contribution to the reaction mechanism and in the larger surface of the notch, with involvement in the transmission mechanism of the axial load only. In negative direction, the model is not capable to reach the same yield point in particular, in terms of force however, the post-elastic behavior showed by numerical results is more stable. The elastic stiffness of the negative rotation show a good agreement considering the heterogeneity obtained in the tests performed, in particular, under 2.5 MPa compression level of the rafter.

The numeric model show to be less effective comparing to the tests results obtained for positive rotation. Nevertheless, it is important to point out that the tests results for both skew angles values analyzed presented significant variations when submitted to positive rotation.

As expected, the results from the numerical model for positive rotation show a higher stiffness than the experimental results due to the regularity in the representation of the facing surfaces, which contrasts the reality of hand-sawn indentations. The reaction mechanism is located in a decreasing portion of the front notch surface. The rotation progress separated the surfaces in the front notch and the connection rapidly moves toward its ultimate behavior mode. Ultimately, only a small contact area remains at the slant.

3.3 Sensitivity study

Experimental results are not always possible to obtained as tests are expensive and time consuming. Therefore, numerical simulations are normally used to extend the study to others parameters as material properties, geometry, load, etc. Parametric studies can be easily carried out and the sensitivity of the response can be assessed with significant benefits for the understanding of the structural response. An extensive sensitivity study was carried out aiming to evaluate the influence of diverse variable, namely, friction coefficient, compression level on the rafter, skew

angle, notch depth, angle of the notch, height of the rafter and wood specie. The main conclusion achieved can be summarized:

– the friction coefficient has influence in the connection response only under negative rotation. The stiffness as slight dependency while the resistance can be significantly affected. This influence decreases over a friction value of 0.5;
– the axial compression stress of the rafter has primary importance in the connection behavior. The connections stiffness is not affected but a higher axial compression stress of the rafters corresponds to a high resistance. The influence seems to be linear and is not affected by the rotational direction;
– the connection behavior is function of the skew angle. The rotational capacity and stiffness of the connection decreases with the skew angle. This dependency is not linear and, in the particular case of connections response under negative rotation, the skew angle increase results in a more fragile behavior;
– the geometry of the rafter, in particular, the height of rafter cross-section, as a significant influence in the connection behavior. Higher cross-section corresponds to resistance and stiffness rising, however, stiffness shows to be less affected under positive rotation;
– in a correct joint geometry definition, the notch depth as influence only in the response under negative rotation. If the connection geometry has a bad definition, as example, a slight deviation of 3 mm is consider in the cutting process of the notch, the influence of the notch depth moves to the positive rotation. In both cases, the notch depth has influence only in the resistant capacity;
– wood species shows to have a minor influence in the connection behavior.

4 CONCLUSIONS

Traditional timber connections, even without any strengthening device, usually have a significant moment-resisting capacity. Test results have showed that this capacity is function of the compression stress applied in the rafter and skew angle. The numeric analysis performed points out that the heights of the rafter, the friction angle are also important.

Strengthening, usually performed by insertion of metal devices, is indispensable for ensuring adequate joint response, in particular, for seismic loading, or in other adverse and unpredictable loading conditions. All strengthening techniques analyzed results in a significant increase of the equivalent viscous damping ratio, higher resistance and significant improvement of the ductility.

REFERENCES

Abaqus 2007. *Abaqus/CAE User's manual*. Version 6.7. ABAQUS, Inc.

Branco, J.M. 2008. *Influence of the joints stiffness in the monotonic and cyclic behavio of traditional timber trusses. Assessment of the efficacy of different strengthening techniques*. Bi-National Ph.D thesis, University of Minho and University of Trento.

Oden, J. & Pires, E. 1983. Nonlocal and nonlinear friction laws and variational principles for contact problems in elasticity. *Journal of Applied Mechanics* 50, 67–73.